Electromagnetic and transverse acoustic modes in semi-infinite Fibonacci superlattices

1989 J. Phys.: Condens. Matter 1 3301

(http://iopscience.iop.org/0953-8984/1/21/001)

J. Phys.: Condens. Matter **1** (1989) 3301–3313. Printed in the UK

Electromagnetic and transverse acoustic modes in semi-infinite Fibonacci superlattices

A P Mayer†
Department of Physics, University of California, Irvine, CA 92717, USA

Received 31 October 1988

Abstract. For a two-component superlattice arranged in the quasi-periodic Fibonacci sequence, the optical reflectivity is calculated as function of the angle of incidence, and its connection with the gap structure of the frequency dispersion of the electromagnetic field is demonstrated. Gap modes as guided waves under boundary conditions corresponding to total reflection are also discussed. For the analogous case of elastic waves of shear horizontal polarisation, the surface spectral function is calculated, which is related to the Brillouin scattering cross section. The shape of this function is dominated by peaks due to localised modes, and it shows self-similar structures.

1. Introduction

The fabrication of superlattices composed of two different types of layers ordered in the Fibonacci sequence, first reported by Merlin *et al* [1], has provided a physical realisation of a one-dimensional quasi-periodic structure. The study of this type of superlattice may on the one hand augment our general knowledge about the properties of quasi-periodic crystal structures, but on the other it has become an interesting field of research on its own. A variety of physical properties have already been studied in these systems, among others also the transmission of TE-polarised light [2–4] and acoustic phonons [5].

In the present investigation, the normal modes of the electromagnetic field for both TE- and TM-polarisation and of the displacement field with shear horizontal polarisation in a Fibonacci superlattice are considered and are treated on the same footing. The electromagnetic problem can in fact be regarded as formally being a special case of its acoustic counterpart, and longitudinal phonons under normal incidence can also be treated in the same way. Concerning the problem of the propagation of light, we extend the results obtained in [2–4] by discussing the gap structure in the ω/θ plane, where ω is the frequency of light and θ the angle of incidence. In particular, we address ourselves to the case of TM-polarised modes, where the Brewster phenomenon occurs [6], causing the frequency gaps to vanish for a certain angle of incidence. As a quantity which is easily accessible experimentally, in which the gap structure can be made visible, we calculate the optical reflectivity of a semi-infinite Fibonacci superlattice as a function of the angle of incidence and discuss the influence of the imaginary parts of the dielectric constants of the two materials.

† Permanent address: Institut für Theoretische Physik II, Westfälische Wilhelms-Universität, D-4400 Münster, Wilhelm-Klemm-Strasse 10, Federal Republic of Germany.

0953-8984/89/213301 + 13 $02.50

A main issue addressed in this paper is the occurrence of modes in a semi-infinite or finite Fibonacci superlattice with frequencies in the gaps of the corresponding infinite structure. The fields associated with them are localised at the surface(s). Experimental evidence for the existence of localised modes in Fibonacci superlattices has been reported by Merlin *et al* [7], and many gap modes have been found in the phonon spectrum of a linear chain and the energy spectrum of a one-dimensional tight-binding model by Nori and Rodriguez [8] under various boundary conditions. In the case of light propagation, we consider a finite or semi-infinite structure covered by metallic overlayers, which are idealised as perfect reflectors. The gap modes in this system correspond to special guided waves. In the analogous acoustic problem, we assume stress-free surfaces to obtain surface acoustic waves. A simple method is devised to find the frequencies of the gap modes for the above mentioned boundary conditions.

The acoustic excitations of an effectively semi-infinite layered elastic medium can be investigated experimentally by means of light scattering. Recently, Raman scattering studies have been performed with quasi-periodic superlattices of Si/Ge [9] and GaAs/AlAs [1, 10, 11] compounds, where the acoustic mismatch is small, the light penetrates deeply into the superlattice and the quasi-periodicity mainly comes into play via the Fibonacci sequence of the elasto-optic coefficients. In contrast to these systems, we have here in view metallic superlattices with large acoustic mismatches that can be investigated by Brillouin scattering under oblique incidence. The scattering cross section is then determined by the acoustic spectral function at and in the vicinity of the surface of the superlattice [12]. For shear horizontal polarisation, the spectral function is calculated at the surface. Its major peaks, seen with low resolution, can be attributed to localised modes, while the gap modes seem to play a minor role for structures occurring on smaller frequency scales. These structures show self-similarity.

2. The gap structure

The propagation of electromagnetic waves in optically isotropic layered media is governed by the wave equations

$$-\varepsilon^{-1}(z)\Delta \boldsymbol{A}(\boldsymbol{x}) = (\omega^2/c_0^2)\boldsymbol{A}(\boldsymbol{x}) \tag{2.1}$$

with the transversality condition

$$\boldsymbol{\nabla} \cdot [\varepsilon(z)\boldsymbol{A}(\boldsymbol{x})] = 0. \tag{2.2}$$

Here, $\boldsymbol{A}$ is the vector potential in a gauge in which the scalar potential vanishes. We choose the z axis to be orthogonal to the plane of stratification. The dielectric constant $\varepsilon(z)$ is assumed to be independent of z within each single layer. The solutions to (2.1) are conveniently constructed by decomposing

$$\boldsymbol{A}(\boldsymbol{x}) = \mathrm{e}^{\mathrm{i}Kx}(A_+^{(j)}\,\mathrm{e}^{\mathrm{i}q_j(z-\xi_j)} + A_-^{(j)}\,\mathrm{e}^{-\mathrm{i}q_j(z-\xi_j)})\hat{y} \tag{2.3}$$

for TE polarisation and

$$\boldsymbol{A}(\boldsymbol{x}) = \mathrm{e}^{\mathrm{i}Kx}(A_+^{(j)}(K\hat{z} - q_j\hat{x})\,\mathrm{e}^{\mathrm{i}q_j(z-\xi_j)} + A_-^{(j)}(K\hat{z} + q_j\hat{x})\,\mathrm{e}^{-\mathrm{i}q_j(z-\xi_j)}) \tag{2.4}$$

for TM polarisation, where

$$q_j^2 = \varepsilon_j \frac{\omega^2}{c_0^2} - K^2. \tag{2.5}$$

Without loss of generality, the in-plane component K of the wavevector is chosen to point into the x direction, and ξ_j denotes the position of the upper boundary of the jth layer. The two-component amplitude vectors (A_+, A_-) for neighbouring layers are related through the boundary conditions at the common interface. This relationship may be expressed in terms of transfer matrices [13].

The propagation of acoustic waves of shear horizontal polarisation in a superlattice built of elastically isotropic layers can be treated in the same manner. The equation of motion for the displacement field $\boldsymbol{u}(\boldsymbol{x})$ is given by [14]

$$-c_t^2(z)(\partial^2/\partial x^2 + \partial^2/\partial z^2)u_y(x, z) = \omega^2 u_y(x, z) \tag{2.6}$$

where the transverse sound velocity $c_t(z)$ is assumed to be constant in each layer. The solution is obtained by the ansatz (2.3), where A has to be replaced by u, and

$$q_j^2 = \omega^2/c_j^2 - K^2. \tag{2.7}$$

The boundary conditions involve, in addition to the transverse sound velocities, also the mass densities ρ_j of the different materials [14]. In fact, the case of TM-polarised light is formally contained in that of shear horizontal acoustic modes in that the transfer matrices for the optical problem can be obtained from those of the acoustic one by setting $\rho_1 = \rho_2$ and replacing the transverse sound velocities by the velocities of the light in the different layers.

The case of acoustic modes polarised in the sagittal plane is more complex in that the solution of the corresponding equation of motion involves four exponentials instead of only two in (2.3) and (2.4) [15]. Consequently, one has to deal with 4×4 matrices. In the special situation of normal incidence, i.e., no x- and y-dependence of the displacement field, the transverse polarisation decouples from the longitudinal one. While the transverse solutions of the equation of motion and boundary conditions are given by the shear horizontal modes in the limit $K = 0$, the longitudinal solutions are obtained by replacing the transverse by the longitudinal sound velocity in the corresponding quantities for the transverse modes.

We now consider a superlattice fabricated of two types of layers, A and B, with thicknesses $|a|$ and $|b|$ in the Fibonacci sequence corresponding to the Nth generation in the recursive generation scheme stratified on a substrate of material A. The transfer matrix $\mathbf{T}(N)$ relating the amplitude vector of the top layer (of material A) to the amplitude vector of the substrate, may be calculated recursively via the relation

$$\mathbf{T}(n+1) = \mathbf{T}(n-1)\mathbf{T}(n). \tag{2.8}$$

As initial values, we may choose the diagonal matrix

$$\mathbf{T}(1) = \begin{pmatrix} e^{iq_A a} & 0 \\ 0 & e^{-iq_A a} \end{pmatrix} \tag{2.9}$$

and for $\mathbf{T}(2)$ the transfer matrix for the elementary unit of the corresponding periodic structure given for both the electromagnetic and the shear horizontal acoustic cases in [16]. The traces $2x_N$ of the transfer matrices $\mathbf{T}(N)$ fulfil the recursion relation

$$x_{n+2} = 2x_{n+1}x_n - x_{n-1}. \tag{2.10}$$

The initial values of this trace map are

$$x_1 = \cos(q_A a)$$

$$x_2 = (1/4\lambda_A\lambda_B)[(\lambda_A + \lambda_B)^2 \cos(q_A a + q_B b) - (\lambda_A - \lambda_B)^2 \cos(q_A a - q_B b)]$$

$$x_3 = (1/4\lambda_A\lambda_B)[(\lambda_A + \lambda_B)^2 \cos(2q_A a + q_B b) - (\lambda_A - \lambda_B)^2 \cos(2q_A a - q_B b)] \tag{2.11}$$

where

$$\lambda_A = q_A \qquad \lambda_B = q_B \tag{2.12}$$

$$\lambda_A = \varepsilon_A q_B \qquad \lambda_B = \varepsilon_B q_A \tag{2.13}$$

for TE- and TM-polarised electromagnetic modes, respectively, and

$$\lambda_A = \rho_B c_B^2 q_B \qquad \lambda_B = \rho_A c_A^2 q_A \tag{2.14}$$

for shear horizontal acoustic modes. The dielectric constants ε_A and ε_B are at this stage assumed to be purely real.

For an infinite Fibonacci superlattice, bounded orbits of the trace map (2.10) correspond to physical solutions of (2.1) or (2.6) [17]. From the known properties of the trace map, it follows that the resulting frequency spectrum is fractal with gaps on all frequency scales. The allowed frequencies correspond to a Cantor set in the ω/K plane of Lebesgues measure zero [17, 18, 19]. In this plane, certain lines can be identified for which the superlattice shows perfect transmission, i.e., the corresponding solutions to the equations of motion are plane-wave-like. These lines are determined by the zeros of the off-diagonal elements of $\mathbf{T}(2)$. This is the case in all three physical systems under consideration, if

$$\omega^2 = c_B^2[K^2 + n^2(\pi^2/b^2)] \tag{2.15}$$

where n is an integer and c_B is the velocity of light or the transverse sound velocity in the B-type layers. The lines determined by (2.15) correspond to perfect transmission in the frequency spectrum of any two-component superlattice with isolated B-type layers of constant thickness b.

The off-diagonal elements of $\mathbf{T}(2)$ also vanish for

$$\lambda_A^2 = \lambda_B^2. \tag{2.16}$$

This equation has a non-trivial solution in the case of shear horizontal acoustic modes, if

$$(\rho_A c_A - \rho_B c_B)(\rho_A c_A^2 - \rho_B c_B^2) > 0 \tag{2.17}$$

and in the case of TM-polarised light, yielding a straight line in the ω/K plane. The perfect transmission on this line is essentially the Brewster phenomenon. Defining the Brewster angle θ_B in the B-type medium in the usual way by

$$K = (\omega/c_B)\sin\theta_B \tag{2.18}$$

we obtain

$$\sin\theta_B = [\varepsilon_A/(\varepsilon_A + \varepsilon_B)]^{1/2} \tag{2.19}$$

for TM-polarised light and

$$\sin\theta_B = c_B[(\rho_A^2 c_A^2 - \rho_B^2 c_B^2)/(\rho_A^2 c_A^4 - \rho_B^2 c_B^4)]^{1/2} \tag{2.20}$$

for shear horizontal acoustic waves. It has been pointed out by Sipe *et al* [6] for TM-

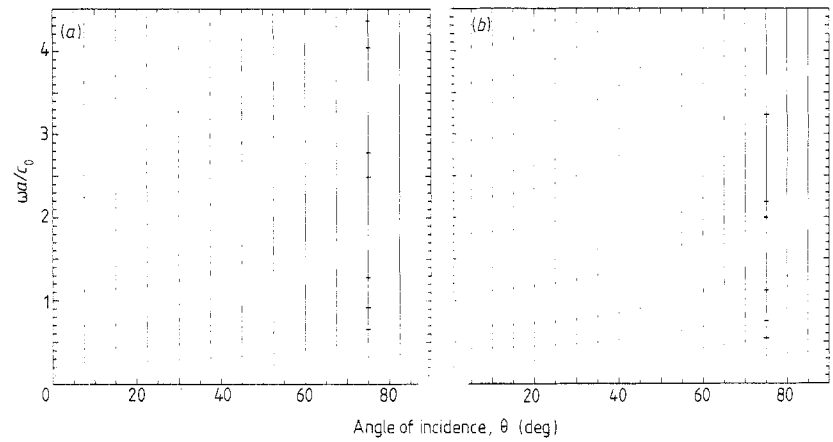

Figure 1. Main frequency gaps (a) for TE-polarised light for 11 different angles of incidence and (b) for TM-polarised light and 17 different angles of incidence in medium B in a Fibonacci superlattice with $a = 0.8303$, $b = 0.5817$, $\varepsilon_A = 16$, $\varepsilon_B = 12$. Of 2000 equidistant points in the frequency interval $0 < \omega < 2\pi c_0/|a + b|$ are plotted those for which $x_{20} > 10^8$. For $\theta = 75°$, the approximate positions of several gap modes are indicated by horizontal bars.

polarised light, that this angle of incidence of perfect transmission is independent of the sequence and thicknesses of the layers in a superlattice fabricated of not more than two materials. This of course also applies to the acoustic case.

The gap structure in the frequency spectrum of optic modes in a Fibonacci superlattice is illustrated in figure 1(a, b). The dielectric constants have been chosen to be in the range of those of germanium and silicon. These diagrams may be regarded as the analogues of the optical band structure for a periodic superlattice [13]. The behaviour of the major gaps as function of the angle θ, where

$$K = \sqrt{\varepsilon_B}(\omega/c_0) \sin \theta \tag{2.21}$$

is remarkably similar in the periodic and quasi-periodic case. In the case of TM polarisation, the gaps shrink to zero at the Brewster angle. At this angle, the transfer matrices $\mathbf{T}(N)$ reduce to

$$\mathbf{T}(N) = \begin{pmatrix} e^{i\zeta_N} & 0 \\ 0 & e^{-i\zeta_N} \end{pmatrix} \tag{2.22}$$

and

$$\zeta_{n+1} = \zeta_n + \zeta_{n-1} \tag{2.23}$$

or, directly,

$$\zeta_n = q_A[F_n a + F_{n-1}(\varepsilon_B/\varepsilon_A)b] \qquad n > 1 \tag{2.24}$$

where F_n are the Fibonacci numbers. The behaviour of this simple map as function of the frequency should determine the multifractal form of the frequency spectrum near the Brewster angle [19].

A qualitative understanding of the resulting gap structure illustrated in figure 1(a, b) can be achieved by applying perturbation theory to (2.1) with respect to the difference in the dielectric constants, starting with plane waves as the unperturbed solutions [10].

The opening of the gaps may then be regarded as the result of lifting the frequency degeneracy of waves with

$$q = \pm\tfrac{1}{2}k_{n,m} \tag{2.25}$$

where

$$k_{n,m} = 2\pi(m + \tau n)/\tau(b + \tau a) \tag{2.26}$$

and

$$\tau = (1 + \sqrt{5})/2 \tag{2.27}$$

is the golden mean. For a sufficiently small difference in the dielectric constants, the mid-frequencies of the gaps for a given angle θ are

$$\omega_{n,m} = c_0 k_{n,m}/2\sqrt{\varepsilon}\cos\theta \tag{2.28}$$

for both TE and TM polarisation, while the gap widths are, within this approximation, given by

$$\Delta\omega_{n,m} = |\varepsilon_B^{-1} - \varepsilon_A^{-1}|\omega_{n,m}|F(k_{n,m})| \tag{2.29}$$

$$\Delta\omega_{n,m} = |\varepsilon_B^{-1} - \varepsilon_A^{-1}|\,|\cos(2\theta)|\omega_{n,m}|F(k_{n,m})| \tag{2.30}$$

for TE and TM polarisation, respectively. Here, ε is the average dielectric constant. The factor $\cos(2\theta)$ in the TM case accounts for the shrinking of the gaps, when the Brewster angle is approached, in the limit $\varepsilon_A = \varepsilon_B$. Using the results of Dharma-wardana *et al* [9], one obtains for the function F:

$$F(k_{n,m}) = \frac{2\tau^2}{b + \tau a}\,\frac{\sin(k_{n,m}a/2)}{k_{n,m}}\,\frac{\sin(z_{n,m}\tau^{-1})}{z_{n,m}}$$

$$z_{n,m} = \pi\tau[(a/b)m - n]/(\tau^{-1} + a/b). \tag{2.31}$$

The corresponding gap positions and widths at a fixed frequency are obtained analogously:

$$\cos\theta_{n,m} = c_0 k_{n,m}/2\sqrt{\varepsilon}\omega \tag{2.32}$$

$$\Delta\theta_{n,m} = 2|\varepsilon_A - \varepsilon_B|\varepsilon^{-1}\,|\sin^{-1}(2\theta_{n,m})|\,|F(k_{n,m})| \tag{2.33}$$

$$\Delta\theta_{n,m} = 2|\varepsilon_A - \varepsilon_B|\varepsilon^{-1}\,|\mathrm{cotan}(2\theta_{n,m})|\,|F(k_{n,m})|. \tag{2.34}$$

For large angles θ, the above formulae do not correctly describe the behaviour of the gaps.

3. The optical reflectivity

As a measurable quantity in which the gap structure of the frequency spectrum of the light becomes directly visible, we discuss the optical reflectivity. We consider a finite Fibonacci superlattice of the Nth generation on a substrate of type A, bounded by a medium M with real dielectric constant ε_M. The ratio R of reflected to incident intensity for light of frequency ω, incident from medium M on the surface of the superlattice with parallel component K of the wavevector, may be calculated using the formula

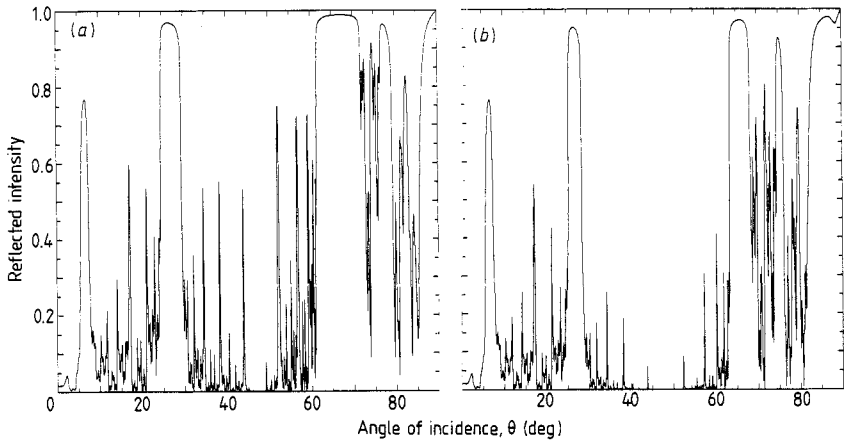

Figure 2. Reflected intensity for (*a*) TE-polarised and (*b*) TM-polarised light incident from an overlayer of material B on the Fibonacci superlattice. Parameters are as in figure 1. Imaginary parts of the dielectric constants: $\varepsilon''_A = 0.01$, $\varepsilon''_B = 0$.

$$R = \left| \frac{T_{11}(N)S_2 + T_{12}(N)S_1}{T_{11}(N)S_1 + T_{12}(N)S_2} \right|^2 \tag{3.1}$$

where

$$S_1 = (q_A + q_M)/2q_A \qquad S_2 = (q_A - q_M)/2q_A \tag{3.2}$$

for TE-polarisation, and

$$S_1 = (\varepsilon_M q_A + \varepsilon_A q_M)/2\varepsilon_A q_A \quad S_2 = (\varepsilon_M q_A - \varepsilon_A q_M)/2\varepsilon_A q_A \tag{3.3}$$

for TM-polarisation. In the case $M = B$, the reflection coefficient R is displayed as a function of angle of incidence in figure 2(*a*, *b*) for the wavelength in vacuum $\lambda = 5.145a$. While ε_B is taken to be real, an imaginary part of 0.01 has been given to ε_A to ensure that the penetration depth of the light is smaller than the extension of the finite superlattice. Consequently, we are effectively dealing with a semi-infinite geometry and avoid resonances due to the finite thickness of the superlattice. By comparison with the reflectivity of a finite periodic superlattice with the same number of A-layers, it has been confirmed that such resonances are in fact absent. The maxima in the reflection coefficient can therefore all be related to frequency gaps. This can be verified by comparing figures 2 and 3. Large gaps appear as higher peaks and smaller gaps as lower peaks. This can be easily understood in the following way. The larger a gap, the faster the traces x_N grow with increasing N, and consequently the smaller the penetration depth of the light in the superlattice and the absorption due to the imaginary part of the dielectric constants. In accordance with this interpretation, the reflectivity peaks become smaller and finally disappear in the neighbourhood of the Brewster angle $\theta_B = 49.1°$ in figure 2(*b*).

With increasing imaginary parts of the dielectric constants, the structures of the curves in figure 2 become more and more smoothed. Figures 4(*a*, *b*) show the reflection coefficient as function of the angle of incidence for a system with medium M chosen as a vacuum and the imaginary parts of ε_A and ε_B both taken as 0.04.

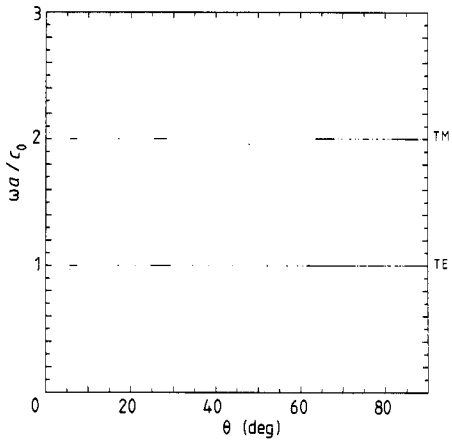

Figure 3. Main gaps for fixed wavelength $\lambda = 5.145a$ of light. Of 2000 equidistant points in the interval $0 < \theta < 90°$ are plotted those for which $x_{20} > 10^8$. Parameters are as in figure 1.

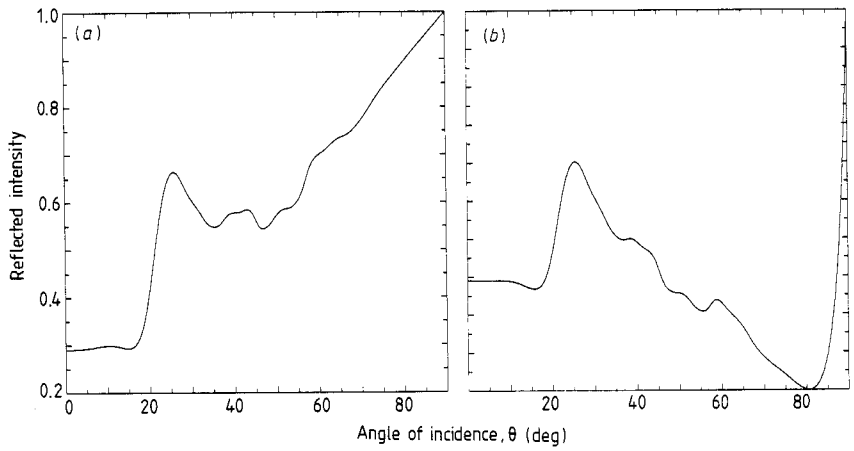

Figure 4. Reflected intensity for (*a*) TE-polarised and (*b*) TM-polarised light, incident from a vacuum. Imaginary parts of the dielectric constants: $\varepsilon''_A = \varepsilon''_B = 0.04$.

4. Gap modes

In a finite or semi-infinite Fibonacci superlattice, there are solutions to the field equations (2.1), (2.2) and (2.6), which do not correspond to a bounded orbit of the trace map, but have their frequencies in the gaps discussed above. The field distribution of these modes is localised at the surfaces of the finite or semi-infinite structure. From the results in [8], the frequencies of these modes are expected to depend strongly on the boundary conditions imposed on the electromagnetic field at the upper and lower surface of the superlattice, as well as on whether the truncation of the sequence of layers in the Fibonacci order takes place after a complete generation or not.

As an example for the case of an optical system, we consider a dielectric Fibonacci superlattice of the complete Nth generation bounded by perfectly reflecting materials. The condition for a guided wave to exist in this system can be cast into the form

$$y_N = 0 \tag{4.1}$$

where

$$y_N^{(\mathrm{TE})} = \frac{1}{2\mathrm{i}}\begin{pmatrix}1\\1\end{pmatrix}\mathbf{T}(N)\begin{pmatrix}1\\-1\end{pmatrix} \tag{4.2}$$

and

$$y_N^{(\mathrm{TM})} = \frac{1}{2\mathrm{i}}\begin{pmatrix}1\\-1\end{pmatrix}\mathbf{T}(N)\begin{pmatrix}1\\1\end{pmatrix} \tag{4.3}$$

for the two different polarisations.

To study gap modes in the analogous acoustic case, we consider a finite Nth generation superlattice with stress-free surfaces. The frequencies of the shear horizontal modes in this structure can be calculated from the equation

$$y_N^{(\mathrm{SH})} = \frac{1}{2\mathrm{i}}\begin{pmatrix}1\\-1\end{pmatrix}\mathbf{T}(N)\begin{pmatrix}1\\1\end{pmatrix} = 0. \tag{4.4}$$

The quantities y_N are real, if q_A is real, otherwise purely imaginary. They obey the recursion relation

$$y_{n+1} = 2x_n y_{n-1} + y_{n-2}. \tag{4.5}$$

The initial values are given by

$$\begin{aligned} y_1 &= \sin(q_A a) \\ y_2 &= (1/2\lambda_B)[(\lambda_A + \lambda_B)\sin(q_A a + q_B b) - (\lambda_A - \lambda_B)\sin(q_A a - q_B b)] \\ y_3 &= (1/4\lambda_A\lambda_B)[(\lambda_A + \lambda_B)^2 \sin(2q_A a + q_B b) - (\lambda_A - \lambda_B)^2 \sin(2q_A a - q_B b) \\ &\quad + 2(\lambda_A^2 - \lambda_B^2)\sin(q_B b)]. \end{aligned} \tag{4.6}$$

Gap modes can then be found by observing changes of the sign of y_N when varying ω or K in regions where the trace map is unbounded. Since the fields of the gap modes are largely localised at the superlattice boundaries, their positions in the ω/K plane will, with increasing N, only depend on whether N is even or odd. In the recursive generation scheme of a Fibonacci superlattice, two different types of structures with equal upper, but different lower ends are built up in alternating sequence with increasing N. Consequently, those gap modes, the positions of which do not change when solving (4.1) for N and $(N+1)$, are expected to be localised at the upper surface, while the others are localised at the lower superlattice surface. The approximate positions of some gap modes in large gaps at $\theta = 75°$, localised at the upper surface, are indicated in figure 1. In principle, localised modes have to be expected in arbitrarily small gaps with a localisation length increasing with decreasing gap width. The magnitude of the localisation length l may be estimated from the values x_N of the trace map, which in the gap regions grow exponentially with the total thickness L_N of the Nth generation superlattice:

$$l \simeq L_N/\ln(2x_N) \tag{4.7}$$

for sufficiently large N.

Note that in this section the equations given for the case of acoustic modes of shear horizontal polarisation again also apply to the case of longitudinal modes with $K = 0$, if the velocity of transverse sound is replaced by that of longitudinal sound.

5. The surface spectral function

The acoustic modes of a semi-infinite layered structure can be investigated experimentally in inelastic scattering experiments. Brillouin scattering has been proved to be particularly adequate for this purpose [20]. The central quantities entering the cross section of a scattering experiment are the spectral functions $S_{\alpha\beta}(z, z', \boldsymbol{K}, \omega)$, which are related to the imaginary part of the elastic Green tensor via

$$S_{\alpha\beta}(z, z', \boldsymbol{K}, \omega) = \omega^{-1} \operatorname{Im}[g_{\alpha\beta}(z, z', \boldsymbol{K}, \omega)] \tag{5.1}$$

in the high temperature limit ($\hbar\omega \ll k_B T$). The shear horizontal modes determine the function $S_{yy}(z, z', [K, 0, 0], \omega)$, which enters the cross section for crossed polarised Brillouin scattering [12]. A detailed quantitative calculation of the Brillouin scattering cross section requires the knowledge of the distribution of the electromagnetic field, in the Fibonacci superlattice, which, as the results in the above sections suggest, will show a complex behaviour in a dielectric structure. In the case of metallic superlattices, however, which we have in view here, the calculation will be simplified considerably if the skin depth for the light is of the order of magnitude of the layer thicknesses. In the special case of the light penetrating only the first layer, or if the mismatch of the dielectric constants is negligibly small, it follows from the general formulae of [21, 12] that the cross section for crossed polarised scattering is given by

$$\frac{\mathrm{d}^2\sigma}{\mathrm{d}\Omega_a\,\mathrm{d}\omega} = \frac{2}{\pi^2} k_B T \left(\frac{\omega}{c_0}\right)^4 \frac{\cos^2\theta}{\cos\theta_0} \frac{|p_0|^2\,|\varepsilon_A|^4}{|p_0 + q_0|^2\,|\varepsilon_A p + q|^2} \int_{-\infty}^{0} \mathrm{d}z \int_{-\infty}^{0} \mathrm{d}z'\, \mathrm{e}^{\mathrm{i}(q^* + q_0^*)z}$$
$$\times \mathrm{e}^{-\mathrm{i}(q+q_0)z'}\, p_{44}^*(z)\, p_{44}(z') \left(-\mathrm{i}q^*(K - K_0) - K\frac{\partial}{\partial z}\right)$$
$$\times \left(\mathrm{i}q(K - K_0) - K\frac{\partial}{\partial z'}\right) S_{yy}(z, z', [K - K_0, 0, 0], \omega - \omega_0) \tag{5.2}$$

where, as in [21], the wavevectors of the incoming light of frequency ω_0 and outgoing light of frequency ω are

$$(K_0, 0, p_0) \qquad \text{and} \qquad (K, 0, p) \tag{5.3}$$

in a vacuum and

$$(K_0, 0, -q_0) \qquad \text{and} \qquad (K, 0, -q) \tag{5.4}$$

in the medium, $p_{44}(z)$ is a Pockels coefficient and θ_0 and θ are the angle of incidence and the scattering angle, respectively.

Using the method outlined in [14], one may express the Green function $g_{yy}(z, z', \boldsymbol{K}, \omega)$ in the first layer of a finite Fibonacci superlattice of the Nth generation in terms of the transfer matrix $\mathbf{T}(N)$:

$$g_{yy}(z, z', \boldsymbol{K}, \omega) = [1/2\mathrm{i}q_A(t_- - t_+)](t_+ \mathrm{e}^{\mathrm{i}q_A(z+z')} + t_- \mathrm{e}^{-\mathrm{i}q_A(z+z')} + t_+ \mathrm{e}^{-\mathrm{i}q_A|z-z'|}$$
$$+ t_- \mathrm{e}^{\mathrm{i}q_A|z-z'|}) \tag{5.5}$$

where

$$t_+ = T_{22}(N) - T_{12}(N) \tag{5.6a}$$

and

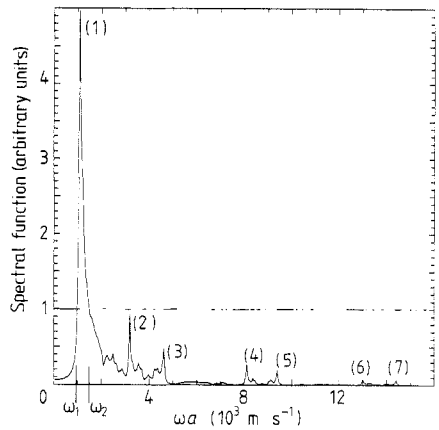

Figure 5. Spectral function $S_{yy}(0, 0, [K, 0, 0], \omega)$ for a Fibonacci superlattice with A/B = Nb/Cu and $Ka = 0.5, a/b = 2$. Parameters as in [14]. Frequency resolution: $\eta a = 40$ m s^{-1}. The approximate positions of the main gaps are marked by horizontal bars. Estimated penetration depths of localised modes in units of a: (1) 43, (2) 21, (3) 19, (4) 10, (5) 10, (6) 14, (7) 14.

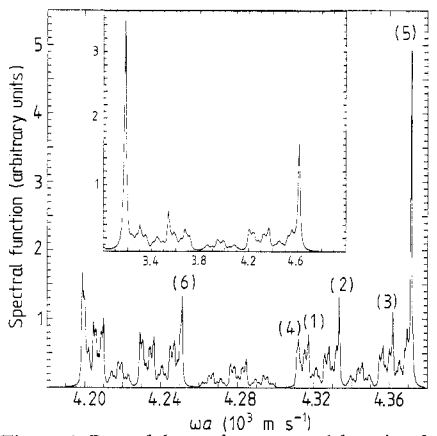

Figure 6. Part of the surface spectral function for the system and geometry of figure 5 with higher resolution ($\eta a = 1.0$ m s^{-1} for the inset and $\eta a = 0.33$ m s^{-1} for the main figure). Estimated penetration depths of the indicated localised modes in units of $1000a$: (1) 5, (2) 2, (3) 3, (4) 9, (5) 0.3, (6) 2.5.

$$t_- = T_{11}(N) - T_{21}(N). \tag{5.6b}$$

As expected, the denominator in (5.5) is proportional to y_N. The spectral function in (5.2) has been calculated numerically at the surface of the superlattice, i.e., for $z = z' = 0$. For sufficiently small skin depth of the light, this function should bear the basic features of the cross section for crossed polarised Brillouin scattering. The system Nb/Cu with $Ka = 0.5$ and $Kb = 0.25$ has been chosen, because of its large acoustical mismatch, and because for this system, a direct comparison with the results of Camley *et al* [14] for the periodic case is possible. In the numerical calculation of the Green function (5.5), a small imaginary part η has been added to the frequency ω. This corresponds to convolving the spectral function with a Lorentzian resolution function of width η. The effect of the imaginary part can also be regarded as introducing a finite penetration depth for the acoustic modes in a way analogous to that of the imaginary part of the dielectric constant for the optic modes. The parameters may then be chosen such that the boundary condition at the lower surface has no influence on the shape of the spectral function at the upper surface. The spectral function for the system under consideration shown in figure 5 is clearly dominated by localised modes. Their penetration depths have been estimated from (4.7) to extend in all cases over a considerable number of layers. They therefore have to be regarded as closely related to the ordering of the layers in the Fibonacci sequence. The high peak in the frequency interval $\omega_1 < \omega < \omega_2$, where q_A is real, while q_B is imaginary, occurs in the spectral function of the corresponding periodic structure at the same position [14]. The penetration depth of the localised mode associated with it is larger in the Fibonacci structure. A characteristic feature of the surface spectral function in figure 5 is the structure bounded by the pair of peaks (2) and (3), which seems to be replicated twice at higher frequencies. A comparison between figures 5 and 6 reveals the self-similarity of the spectral function in this frequency range with the reproduction of a characteristic triple structure on smaller frequency

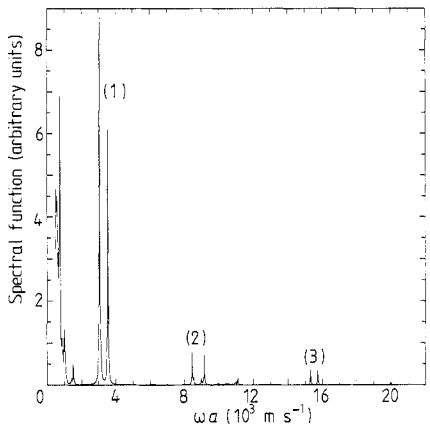

Figure 7. Spectral function $S_{zz}(0, 0, [0, 0, 0], \omega)$ for a Fibonacci superlattice with A/B = Al/W. Mass densities and longitudinal sound velocities are as in [15]. Frequency resolution: $\eta a = 20\ \mathrm{m\ s^{-1}}$.

scales [22, 23]. Further localised modes have been found on the frequency scale of figure 6, as indicated, in smaller gaps with consequently larger penetration depths. Localised modes have in fact to be expected in gaps of arbitrarily small width. The peak positions in figure 6, however, no longer always coincide precisely with the frequency of gap modes. With decreasing gap width and thus increasing delocalisation of the corresponding gap modes, the latter become less important for the surface spectral function, and those modes that correspond to bounded orbits of the trace map gain increasing influence on the structure of the spectral function on smaller frequency scales.

Finally, we give an example for the spectral function $S_{zz}(0, 0, \mathbf{0}, \omega)$, which is determined by the longitudinal modes with $\boldsymbol{K} = 0$. This function is directly proportional to the contribution of pure ripple scattering from the surface of the superlattice to the Brillouin scattering cross section for normal incidence and zero scattering angle. In the system Al/W we have chosen here, this scattering mechanism is expected to be the dominant one. The acoustic modes of sagittal polarisation for periodic superlattices of these materials with a large acoustic mismatch have been investigated in [15]. In figure 7 the surface spectral function for the corresponding Fibonacci sequence of layers is shown with $a/b = 2$. The three pairs of peaks marked (1), (2) and (3) can again be identified as resulting from localised modes in frequency gaps.

It is hoped that the theoretical results presented here will give rise to further experimental investigations of quasi-periodic superlattices, in particular light-scattering experiments on metallic Fibonacci structures. For a full theoretical evaluation of the Brillouin scattering cross section for non-zero angle of incidence or scattering angle and arbitrary polarisation of the incident and scattered light, the acoustic modes of sagittal polarisation have to be taken into account. Since they are associated with 4×4 instead of 2×2 transfer matrices, the concepts used in the above analysis are not directly applicable, and new interesting features may be expected in physical quantities related to them.

Acknowledgments

The author would like to thank Professors A A Maradudin, D L Mills and Dr B Hillebrands for stimulating discussions, the Physics Department of UC Irvine for its hospitality and the Deutsche Forschungsgemeinschaft for financial support.

References

[1] Merlin R, Bajema K, Clarke R, Juang F-Y and Bhattacharya P K 1985 *Phys. Rev. Lett.* **55** 1768
[2] Kohmoto M, Sutherland B and Iguchi K 1987 *Phys. Rev. Lett.* **58** 2436
[3] Würtz D, Schneider T and Soerensen M P 1987 *Preprint*
[4] Dutta Gupta S and Shankar Ray D 1988 *Phys. Rev.* B **38** 3628
[5] Tamura S and Wolfe J P 1987 *Phys. Rev.* B **36** 3491
[6] Sipe J E, Ping Sheng, White B S and Cohen M H 1988 *Phys. Rev. Lett.* **60** 108
[7] Merlin R, Bajema K, Mullen K, Ben-Jacob E, Juang F-Y and Bhattacharya P 1986 *Bull. Am. Phys. Soc.* **31** 348
[8] Nori F and Rodriguez J P 1986 *Phys. Rev.* B **34** 2207
[9] Dharma-wardana M W C, MacDonald A H, Lockwood D J, Baribeau J-M and Houghton D C 1987 *Phys. Rev. Lett.* **58** 1761
[10] Lockwood D J, MacDonald A H, Aers G C, Dharma-wardana M W C, Devine R L S and Moore W T 1987 *Phys. Rev.* B **36** 9286
[11] Bajema K and Merlin R 1987 *Phys. Rev.* B **36** 4555
[12] Mills D L, Maradudin A A and Burstein E 1970 *Ann. Phys.* **56** 504
Bennett B I, Maradudin A A and Swanson L R 1972 *Ann. Phys.* **71** 357
[13] Yeh P, Yariv A and Hong Chi-Shain 1977 *J. Opt. Soc. Am.* **67** 423
[14] Camley R E, Djafari-Rouhani B, Dobrzynski L and Maradudin A A 1983 *Phys. Rev.* B **27** 7318
[15] Djafari-Rouhani B, Dobrzynski L, Hardouin Duparc O, Camley R E and Maradudin A A 1983 *Phys. Rev.* B **28** 1711
[16] Mayer A P to be published
[17] Kohmoto M, Kadanoff L P and Tang C 1983 *Phys. Rev. Lett.* **50** 1870
[18] Kadanoff L P and Tang C 1984 *Proc. Nat. Acad. Sci. USA* **81** 1276
[19] Kohmoto M and Oono Y 1984 *Phys. Lett.* **102A** 145
[20] Sandercock J R 1970 *Opt. Commun.* **2** 73
[21] Marvin A, Bortolani V and Nizzoli F 1980 *J. Phys. C: Solid State Phys.* **13** 299
[22] Lu Jian Ping, Odagaki T and Birman J L 1986 *Phys. Rev.* B **33** 4809
[23] Niu Q and Nori F 1986 *Phys. Rev. Lett.* **57** 2057